Targeting TNF/IL-17/MAPK pathway in h*E2A-PBX1* leukemia: effects of OUL35, KJ-Pyr-9, and CID44216842

Haiping Luo,[1*] Qiqi Li,[1*] Jiaxin Hong,[1] Zhibin Huang,[1] Wenhui Deng,[1] Kunpeng Wei,[1] Siyu Lu,[1] Hailong Wang,[2] Wenqing Zhang[1] and Wei Liu[1]

[1]Division of Cell, Developmental and Integrative Biology, School of Medicine, South China University of Technology and [2]KingMed School of Laboratory Medicine, Guangzhou Medical University, Department of Basic Research, Guangzhou Laboratory, Guangzhou, China

[*]*HL and QL contributed equally as first authors.*

Correspondence: W. Liu
liuwei7@scut.edu.cn

W. Zhang
mczhangwq@scut.edu.cn

Received: June 13, 2023.
Accepted: February 12, 2024.
Early view: February 22, 2024.

https://doi.org/10.3324/haematol.2023.283647

Abstract

t(1;19)(q23;p13) is one of the most common translocation genes in childhood acute lymphoblastic leukemia (ALL) and is also present in acute myeloid leukemia (AML) and mixed-phenotype acute leukemia (MPAL). This translocation results in the formation of the oncogenic E2A-PBX1 fusion protein, which contains a trans-activating domain from E2A and a DNA-binding homologous domain from PBX1. Despite its clear oncogenic potential, the pathogenesis of E2A-PBX1 fusion protein is not fully understood (especially in leukemias other than ALL), and effective targeted clinical therapies have not been developed. To address this, we established a stable and heritable zebrafish line expressing human *E2A-PBX1 (hE2A-PBX1)* for high-throughput drug screening. Blood phenotype analysis showed that h*E2A-PBX1* expression induced myeloid hyperplasia by increasing myeloid differentiation propensity of hematopoietic stem cells (HSPC) and myeloid proliferation in larvae, and progressed to AML in adults. Mechanistic studies revealed that hE2A-PBX1 activated the TNF/IL-17/MAPK signaling pathway in blood cells and induced myeloid hyperplasia by upregulating the expression of *runx1*. Interestingly, through high-throughput drug screening, three small molecules targeting the TNF/IL-17/MAPK signaling pathway were identified, including OUL35, KJ-Pyr-9, and CID44216842, which not only alleviated the hE2A-PBX1-induced myeloid hyperplasia in zebrafish but also inhibited the growth and oncogenicity of human pre-B ALL cells with E2A-PBX1. Overall, this study provides a novel h*E2A-PBX1* transgenic zebrafish leukemia model and identifies potential targeted therapeutic drugs, which may offer new insights into the treatment of E2A-PBX1 leukemia.

Supplemental Information

Supplementary Materials and Methods

Fish care and strains

The zebrafish used in the experiment were all from the zebrafish breeding system of South China University of Technology. Zebrafish were raised, bred, and staged according to standard protocols[1]. The following lines were used: wild type (WT), hematopoiesis-defective zebrafish mutant (*runx1*^{w84x})[2], *Tg(lyz: DsRed)*[3], *Tg(rag2:DsRed)*[4].

Adult zebrafish and embryos heat-shock treatment

We induced the expression of human *E2A-PBX1* (h*E2A-PBX1*) in *Tg(hsp70: E2A-PBX1-EGFP)* zebrafish by heat shock to explore its influence on the hematopoietic development of zebrafish. Zebrafish larvae were subjected to 39.5 ℃ heat shock at 12 hpf for 1 h, then were subjected to heat shock twice a day at 39.5 ℃ for 2 h each time. Adult fish were subjected to heat shock twice daily at 39.5 ℃ for 2 h each time.

RT-qPCR

Total RNA was extracted from embryos using TRIZOL reagent (Invitrogen) according to the instructions[5]. The RT-qPCR primers are listed in Table S2.

Morpholino oligonucleotides

Antisense morpholino oligonucleotide (MO) named *runx1* MO was obtained from Gene Tools. *runx1* Morpholino sequences[2]：5’-TGTTAAACTCACGTCGTGGCTCTC-3’. The control group was treated with 0.2, 0.5, and 0.7 mM random sequences MO.

Genotyping

Tg(hsp70: E2A-PBX1-EGFP) transgenic zebrafish were identified by PCR using h*E2A-PBX1* transgene-specific primers 5′-GGCAGGTTCAGACAACTCAGTG-3′ and 5′-AGCTGCATCTGGATGGAGCTG-3′, amplified a 231 bp fragment within the *PBX1* section. DNA polymerase (Transgene) was used with amplification conditions of denaturation at 94℃ for 5 mins, 35 cycles at 94℃ for 30 seconds, 58℃ for 30 seconds, and 72℃ for 30 seconds. *runx1*^{w84x} mutants were identified by PCR using *runx1*-specific primers 5′-TGGTGGGCAAACTGCGCATG-3′ and 5′-TTCTTGCTGTGACACTGAGC-3′, and amplified a 230 bp fragment. DNA polymerase (Transgene) was used with amplification

conditions of denaturation at 94℃ for 5 mins, 35 cycles at 94℃ for 30 seconds, 58℃ for 30 seconds, and 72℃ for 30 seconds and then digested with restriction enzymes HaeII (New England Biolabs), wild type (WT) fragment: 80 bp + 150 bp; mutant fragment: 230 bp.

Whole-mount in situ hybridization (WISH)

WISH was performed essentially as described, for *cebp1, lyz, myb, mpx, mfap4, βe1-globin, rag1,* and *runx1* probes. Their cRNAs were transcribed in vitro by T3 or T7 polymerase (Thermo Fisher Scientific) with a digoxigenin-labeled NTP mix (Roche). Staged embryos were fixed in 4% paraformaldehyde (PFA; Macklin Biotechnology) for whole-mount in situ hybridization (WISH) with probes according to standard protocols[6].

May-Grunwald Giemsa staining

May-Grunwald Giemsa (Sigma) staining was performed as described previously[7].

Sudan Black B (SB) staining

SB staining was performed according to a previous report[8].

Cell cultures and labeling

Human B-ALL *E2A-PBX1*(+) RCH-ACV cells grew in RPMI 1640 medium (Gibco™) with 10% (vol/vol) fetal bovine serum (Biological Industries). All cells were labeled with Cell Plasma Membrane Staining Kit with DiI (Red Fluorescence; Beyotime Biotechnology), a lipophilic fluorescent tracking dye according to the manufacturer's instructions. 10 μM Dil was applied to the cells for 20 mins at RT[9].

CCK8 assay

Cell viability was analyzed by Cell Counting Kit-8 (CCK8, Beyotime, Shanghai, China) according to the manufacturer's protocols and a previous report[10]. Cells were seeded and cultured at a density of 1×10^4/mL in 100 μL of medium into 96-well microplates (Corning, USA). Then, the cells were treated with various concentrations of Cytarabine (0, 1, 5, and 10 μM), CID44216842 (0, 5, 10 and 30 μM), KJ-Pyr-9 (0, 3, 10 and 20 μM)and OUL35 (0, 1, 5 and 10 μM). After treatment for 60 hours, 10 μL of CCK-8 reagent was added to each well and then cultured for 6 hours. And followed by detection at 450 nm.

Cell TUNEL assay

We collected cells and performed the TUNEL assay according to the instructions (In Situ Cell Death Detection Kit; Roche). Briefly, we fixed the collected cells with 4% PFA for 30 minutes after centrifugation. Washing three times with PBS (5 minutes each time) and digesting with 0.5% Triton-X-100 for 5 minutes, and then washing three times with PBS. Preparing the TUNEL reaction mixture, mix 50 μL TdT with 450 μL fluorescently labeled dUTP for the treatment group. After the slides are dry, add 50 μl of the TUNEL reaction mixture to each sample. Wash three times with PBS (5 minutes each time) adding DAPI staining solution and incubate for 15 minutes. Wash three times with PBS (5 minutes each time) and observe the staining results under a microscope.

Adult zebrafish drug treatment

The 15-month-old adult fish, which had been subjected to heat shock for three months, were randomly divided into groups. Each group consisted of six fish, and intraperitoneal injections were administered using a micropipette. The h*E2A-PBX1* transgenic fish were subjected to intraperitoneal injections of the DMSO, Cytarabine (8000 mg/kg), CID44216842 (125 mg/kg), KJ-Pyr-9 (90 mg/kg), and OUL35 (150 mg/kg), and WT zebrafish treated with DMSO. The drug was administered once daily for five consecutive days. On the fifth day of drug administration, PB and KM samples were collected and stained with Giemsa solution.

Western blot

Protein was extracted from whole embryos at 6 days post-fertilization (dpf) after 48 h drug treatment. Proteins were quantified, and assessed by western blot analysis. Protein lysates were probed with mouse anti-p-P38 antibody (1:2000 dilution, Santa Cruz Biotechnology), rabbit anti-P38 antibody (1:1000 dilution, Cell Signaling Technology), rabbit anti-p-Erk1/2 antibody (1:1000 dilution, Cell Signaling Technology), rabbit anti-Erk1/2 antibody (1:1000 dilution, Cell Signaling Technology), rabbit anti-p-Jnk antibody (1:1000 dilution, Cell Signaling Technology), rabbit anti-Jnk antibody (1:1000 dilution, Cell Signaling Technology). Mouse anti-glyceraldehyde 3-phosphate dehydrogenase (GAPDH) antibody (1:5000 dilution, Cell Signaling Technology) was included as an internal control.

Transplantation

Whole KM cell suspensions were prepared from *Tg(lyz: DsRed)* and *Tg(hsp70:E2A-PBX1-EGFP;lyz: DsRed)* (AML-like) fish. 2.6×10^5 cells were injected periophthalmically into fonx1/Casper recipients using a glass capillary needle (World Precision Instruments). fonx1/Casper zebrafish are cultured in a sterile system.

Inhibitor treatment

TNF-α inhibitors pomalidomide (MedChemExpress) and lenalidomide (MedChemExpress), as well as IL-17 inhibitor Y-320 (MedChemExpress) were commercially acquired and utilized following the manufacturer's instructions.

Supplemental Tables

Table S1 Information of seven small-molecule compounds

Name	Pathways	Target	Bioactivity	references
KJ-Pyr-9	Autophagy; CellCycle/Checkpoint	Autophagy; c-Myc	KJ Pyr 9 is an MYC inhibitor	[10]
OUL35	Chromatin/Epigenetic; DNA Damage/DNA Repair	PARP	OUL35 is a selective PARP-10 inhibitor, and small-molecule ARTD10 inhibitor. OUL35 has been shown to rescue cells from ARTD10-induced cell death.	[11, 12]
L-Arginine hydrochloride	Immunology/Inflammation; Metabolism	Amino Acids and Derivatives; Endogenous Metabolite; NO Synthase	L-Arginine is a nitrogen donor for synthesis of nitric oxide, can be used in the study of functional dyspepsia such as upper digestive tract dysfunction or dysfunction	[13]
A-484954	Autophagy; Microbiology/virology; Neuroscience	Autophagy; CaMK; Parasite	A 484954 is a highly specific eukaryotic elongation factor-2 (eEF2, IC50: 280 nM) inhibitor.	[14]
CID44216842	CellCycle/Checkpoint; GPCR/G Protein; MAPK	CDK; Ras	CID44216842 is a potent Cdc42-selective guanine nucleotide binding lead inhibitor. It is also a Ras protein inhibitor.	[15, 16]
GLPG1837	Autophagy; Membrane transporter/Ion channel	Autophagy; CFTR	an effective CFTR potentiator	[17]
LRRK2-IN-1	Apoptosis; Autophagy; CellCycle/Checkpoint	Apoptosis; CDK; LRRK2	an effective and selective LRRK2 inhibitor	[18]

Table S2 RT-qPCR primer sequence

gene	forward primer	reverse primer	reference
PBX1	GGCAGGTTCAGACAACTCAGTG	AGCTGCATCTGGATGGAGCTG	This paper
runx1	GTAGCAAAGTCACCTTACAG	GAAACTCCCTCATACACCA	This paper
socs3b	AGTGCGATTCCTCCTCCTTT	GGCTGAGGGCATGTAATGAT	[19]
fosab	TTACCAGCCTTAACGCCGAC	TGGACCATCCACTGCAAGTC	[20]
hsp27	CGGATCCATGGCCGAGAGACGCAT	TTATTTTGTGGTGCTGACGG	[21]
junb	GACCTGCACAAGATGAACCACG	ACTGCTGAGGTTGGTGTAGACG	[22]
mmp9	TGATGTGCTTGGACCACGTAA	ACAGGAGCACCTTGCCTTTTC	[23]
fosb	GGGATGATGCAGGAGAGGGA	GCAAGAAGCGAGGGTGAGTT	[24]
fosl1a	CTCAGCCCTCCCAATCACATCT	TACACTTCGCCGCAGCCATT	[25]
elf1a	TACTTCTCAGGCTGACTGTG	ATCTTCTTGATGTATGCGCT	This paper
mpx	AGAGACTGATAGAGATTCCATCC	CGAACACCACAACTTTAGCA	This paper
tcf3a	GTTCAGAAGCAAACAGTCCTTC	AGAAGCTGCGATGTTGATCTC	This paper
tcf3b	CAGCTCAGGTGACGAGATTG	TGCAATGCCTTGAGGAGAGC	This paper
rag1	AATGATGCAAGGCAGAGGA	CAATGATGCCCACATCCC	This paper
cebpα	CTGCCTGAACGGCTACATGG	GCGTGGTGTTGAGAGTGGT	This paper
pu.1	GTCAGAACGATCACTCTTGG	GTAAGTCATCTGTGGATTGGT	This paper
cebp1	ACACATAGCCATGTCGGT	CTCAGTGTTGGTGTTTGGG	This paper

Table S3 abbreviations

hE2A-PBX1	human E2A-PBX1
ALL	acute lymphoblastic leukemia
AML	acute myelocytic leukemia
dpf	days post fertilization
hpf	hours post fertilization
MO	Morpholino
SB	Sudan Black B

PCR	polymerase chain reaction
CHT	caudal hematopoietic tissue
PFA	paraformaldehyde
PCV	posterior cardinal vein
DA	Dorsal Aorta
HSPCs	hematopoietic stem cells
MRD	Minimal Residual Disease

Supplemental excel 1

Information on 560 small molecule inhibitors (TargetMol's Bioactive Compound Library) for drug screening in hE2A-PBX1 zebrafish.

Supplementary Figure Legends

Figure S1 Humanized transgenic zebrafish express human *E2A-PBX1 (*h*E2A-PBX1)* at 24 hours post-fertilization (hpf). Zebrafish expressing human *E2A-PBX1* were generated by co-injecting *Tol2* mRNA and plasmids into WT embryos. (B) RT-qPCR analysis showed no significant change in *tcf3a* and *tcf3b* mRNA expression in *Tg(hsp70:E2A-PBX1-EGFP)* compared to the sibling controls at 3 dpf. The black asterisks indicate statistical differences (Student's t-tests, mean±SEM, ns: no significance). (C) RT-qPCR analysis showed no significant change in *tcf3a* and *tcf3b* mRNA expression in *Tg(hsp70:E2A-PBX1-EGFP)* compared to the sibling controls at 5 dpf. The black asterisks indicate statistical differences (Student's t-tests, mean±SEM, ns: no significance). (D) RT-qPCR analysis showed no significant change in *tcf3a* and *tcf3b* mRNA expression in *Tg(hsp70:E2A-PBX1-EGFP)* compared to the WT controls at 3 months old after 2 months heat shock. The black asterisks indicate statistical differences (Student's t-tests, mean±SEM, ns: no significance).

Figure S2 Induction of hE2A-PBX1 expression in zebrafish larvae leads to myeloid cell expansion. (A) Whole-mount in situ hybridization (WISH) of *cebp1* and *lyz* expressions in *Tg(hsp70:E2A-PBX1-EGFP)* (right panel) were higher than siblings (left panel) at 3 dpf. The number of lyz-DsRed^{+} cells (caudal hematopoietic tissue (CHT) region and Sudan Black B positive (SB^{+}) cells in *Tg(hsp70:E2A-PBX1-EGFP)* (right) was higher than siblings (left) at 3 dpf. The caudal hematopoietic tissue (CHT) is enlarged in the red box (Original magnification ×200). (A') Statistical analysis of the positive signals (*cebp1, lyz,* lyz-DsRed, and SB) in figure A. The black asterisks indicate statistical difference (Student's t-tests, mean±SEM, *P<0.05, **P<0.01, ***P<0.001, ****P<0.0001) (B) WISH of *rag1* expressions in *Tg(hsp70:E2A-PBX1-EGFP*) (right panel)have a decrease compared to siblings (left panel) at 3 dpf. The number of Rag2-DsRed^{+} cells in *Tg(hsp70: E2A-PBX1-EGFP)* (right panel) has a decrease compared to controls (left panel) at 8 dpf. (B') Statistical analysis of the positive area of *rag1* and Rag2-DsRed in figure B. The black asterisks indicate statistical difference (Student's t-tests, mean ± SEM, **P<0.01, ***P<0.001). (C) WISH of *βe1* expressions in siblings (n=27) (left panel) and *Tg(hsp70: E2A-PBX1-EGFP)* (n=26) (right panel) at 3 dpf.

(C') Statistical analysis of the positive area of *βe1* in figure C. The black asterisks indicate statistical difference (Student's t-tests, mean ± SEM, ns: no significance). n/n, number of zebrafish larvae showing representative phenotype/total number of zebrafish larvae examined.

Figure S3 hE2A-PBX1 induces obvious reduction of lymphocytes in zebrafish larvae. (A) Immunofluorescence double staining of Rag2-DsRed and BrdU antibodies reveals a significant decrease in lymphocytes proliferation in thymus region of 6 dpf *Tg(hsp70:E2A-PBX1-EGFP)* larvae (n=23) compared with the siblings (n=20). Rag2-DsRed/BrdU double-positive cells are indicated by white arrows. (A') Statistical analysis of the percentage of Rag2-DsRed$^+$ BrdU$^+$ cells in figure A. The black asterisks indicate statistical difference (Student's *t*-tests, mean±SEM, *P<0.05). (B) Co-staining of Rag2-DsRed and transferase dUTP nick end labeling (TUNEL) was used to detect the apoptosis in the thymus region of 6 dpf *Tg(hsp70:E2A-PBX1-EGFP)* larvae (n=16) compared with the siblings (n=17). Rag2-DsRed/TUNEL double-positive cells are indicated by white arrows. (B') Statistical analysis of the percentage of Rag2-DsRed$^+$ TUNEL$^+$ cells in figure B. The black asterisks indicate statistical difference (Student's *t*-tests, mean±SEM, ns: not significance). (C) SB staining of sibling and *Tg(hsp70:E2A-PBX1-EGFP)* larvae from 5 dpf (0 day post treatment) to 12dpf (7 days post treatment) after drug treatment with heat shock. The control group sibling was treated with DMSO, the *Tg(hsp70:E2A-PBX1-EGFP)* received treatments with DMSO, 1.5mg/mL Cytarabine, 1.5 μM Flavopiridol. (C') Statistical analysis of the SB$^+$ signals shown in figure C. The black asterisks indicate statistical difference ($n \geqslant 19$, one-way ANOVA, mean±SEM, *P < 0.05, ***P < 0.001, ****P < 0.0001). (D) Survival curves of sibling and *Tg(hsp70:E2A-PBX1-EGFP)* larvae from 5 dpf (0 day post treatment) to 12dpf (7 days post treatment) after drug treatment with heat shock. The black asterisks indicate statistical differences (log-rank (Mantel-Cox) test, *P < 0.05, **P < 0.01).

Figure S4 h*E2A-PBX1* adult fish display abnormal myeloid cell expansion resembled human myeloid pre-leukemia-like phenotypes (A) May-Grunwald-Giemsa staining of peripheral blood (PB) cells (upper panels) and kidney marrow (KM) blood cells (lower panels) in 4-months WT (left panel) and *Tg(hsp70:E2A-PBX1-EGFP)* (right panel) adult fish after

1-month heat shock. Red arrows indicate myelocytes, and black arrows indicate lymphocytes. Original magnification ×400. Blood cell counts of PB and KM were calculated manually based on their morphology. (A') Statistical analysis of cell counts in figure A. The black asterisks indicate statistical difference (n = 11, one-way ANOVA, mean ± SEM, ns: no significance, *P < 0.05). (B) May-Grunwald-Giemsa staining of PB cells (upper panels) and KM blood cells (lower panels) in 6-months WT (left panel) and *Tg(hsp70:E2A-PBX1-EGFP)* (right panel) adult fish after 3-months heat shock. Red arrows indicate myelocytes, black arrows indicate lymphocytes and green arrows indicate blast cells. Original magnification ×400. Blood cell counts of PB and KM were calculated manually based on their morphology. (A') Statistical analysis of cell counts in figure A. The black asterisks indicate statistical difference (n ⩾ 10, one-way ANOVA, mean±SEM, ns: no significance, *P< 0.05). (C) RT-qPCR analysis showed a significant decrease in *rag1* mRNA expression and a significant increase in *cebp1, pu.1, cebpα* and *mpx* mRNA expression in *Tg(hsp70:E2A-PBX1-EGFP)* compared to the WT controls at 15-months old. The black asterisks indicate statistical difference (Student's t-tests, mean±SEM, *P < 0.05, **P < 0.01, ****P < 0.0001).

Figure. S5 *Tg(hsp70:E2A-PBX1-EGFP;Lyz:DsRed)* transgenic cells with induced AML-like disease were transplantable. (A) Immunofluorescent staining of the myeloid-specific marker Lcp1 in frozen sections confirmed myeloid cell infiltration of the skeletal musculature in 6-months WT (upper panels) and *Tg(hsp70:E2A-PBX1-EGFP)* (lower panels) adult fish after 3-months heat shock (yellow arrows show invasion areas of myeloid cells into muscle tissue). (B) Imaging of dying *Tg(hsp70:E2A-PBX1-EGFP;Lyz:DsRed)* at 15 month-old after 3-months heat shock reveals myeloid cell systemic invasion. n/n, number of zebrafish larvae showing systemic invasion/total number of zebrafish larvae examined. (C) Fluorescent images of kidney (left panel), liver (middle panel), and spleen (right panel) labeled with Lyz-Dsred in 1-years *Tg(Lyz:DsRed)* (upper panels) and *Tg(hsp70:E2A-PBX1-EGFP;Lyz:DsRed)* (lower panels) adult fish after 3-months heat shock. White arrows indicate Lyz-Dsred+ myelocytes. Kidey original magnification ×400, liver, and spleen original magnification ×200. (D) *Tg(Lyz:DsRed)* (left panel) and *Tg(hsp70:E2A-PBX1-EGFP;Lyz:DsRed)* (right panel) donor KM blood smears for

transplantation. Green arrows indicate blast cells. Original magnification ×400.

Figure S6 Alleviating the hE2A-PBX1-induced myeloid hyperplasia through reduction of *runx1* expression in zebrafish larvae. (A) WISH of *lyz* expressions in zebrafish larve at 3 dpf. We obtained *Tg(hsp70:E2A-PBX1-EGFP); runx1*^{w84x} by crossing the *Tg(hsp70:E2A-PBX1-EGFP)* with the *runx1* loss-of-function mutants (*runx1*^{w84x}) and identified by PCR and restriction enzyme HaeII. The caudal hematopoietic tissue (CHT) is enlarged in the red box (Original magnification ×200). (A') Statistical analysis of the *lyz*$^{+}$ signals is shown in figure A. The black asterisks indicate statistical difference (n ⩾ 12, one-way ANOVA, mean ± SEM, ****P < 0.0001). (B) Decreased number of *lyz*$^{+}$ neutrophils in sibling and *Tg(hsp70:E2A-PBX1-EGFP)* larvae after injecting 0.7 mM *runx1* morpholino (MO) at 3 dpf. The control groups were treated with 0.7 mM random sequence MO. The caudal hematopoietic tissue (CHT) is enlarged in the red box (Original magnification ×200). (B') Statistical analysis of the *lyz*$^{+}$ signals is shown in figure B. The black asterisks indicate statistical difference (n ⩾ 9, one-way ANOVA, mean ± SEM, ***P < 0.001, ****P < 0.0001). (C) Survival curves of sibling, *Tg(hsp70:E2A-PBX1-EGFP), Tg(hsp70:E2A-PBX1; runx1*$^{+/-}$*)* and *Tg(hsp70:E2A-PBX1-EGFP; hsp70:myc-runx1)* larvae up to 14 days after heat shock. The black asterisks indicate statistical difference (log-rank (Mantel-Cox) test, **P < 0.01).

Figure S7 Small molecule compounds cid44216842 and OUL35 can significantly rescue the mortality of transgenic juvenile fish within 12 days.

(A) Abnormality rate of sibling embryos treated with DMSO, 6.17 mM Ara-C (citicoline), 8 μM KJ-Pyr-9, 20 μM CID44216842 and 24 μM OUL35 at 6 dpf (one-way ANOVA, mean±SEM, ***P < 0.001). (B) Wright-Giemsa staining of whole blood cells from *WT* and *Tg(hsp70:E2A-PBX1-EGF)* after drug treatment at 15 month-old with 3 months heat shock. WT zebrafish were treated with DMSO as control, h*E2A-PBX1* zebrafish were treated with DMSO, Cytarabine (8000 mg/kg), CID44216842 (125 mg/kg), KJ-Pyr-9 (90 mg/kg), and OUL35 (150 mg/kg) respectively. Red arrows indicate myelocytes, black arrows indicate lymphocytes and green arrows indicate blast cells. Original magnification ×400. Blood cell

counts of PB and KM were calculated manually based on their morphology. (B') Statistical analysis of the cell counts in figure B'. The black asterisks indicate statistical difference (one-way ANOVA, mean±SEM, *P<0.05). (C) Survival curves of sibling and *Tg(hsp70:E2A-PBX1-EGFP)* larvae from 5 dpf (0 day post treatment) to 12dpf (7 days post treatment) after drug treatment with heat shock. The control group sibling was given DMSO, the *Tg(hsp70:E2A-PBX1-EGFP)* were treated with DMSO, 1.5mg/mL Cytarabine, 3.0 μMCID44216842, 0.75 μM KJ-Pyr-9 and 20 μM OUL35. The black asterisks indicate statistical differences (log-rank (Mantel-Cox) test, *P < 0.05, **P < 0.01). (D) Effects of TNF inhibitor (pomalidomide and lenalidomide) and IL-17 inhibitor (Y-320) on MAPK phosphorylation in h*E2A-PBX1* zebrafish detected by western blot at 6 dpf. h*E2A-PBX1* zebrafish embryos were collected at 4 dpf and treated with DMSO, 500 μM pomalidomide, 500 μM lenalidomide, and 0.75 μM Y-320 inhibitor, respectively. After 48 hours of treatment (6 dpf), the embryos were collected to detect the phosphorylation levels of MAPK signaling pathway genes. (D') Statistical analysis of the cell counts in figure D'. The black asterisks indicate statistical difference (one-way ANOVA, ns: no significance).

Figure S8 KJ-Pyr-9, OUL35, and CID44216842 inhibited RCH-ACV cells growth in vitro. (A) Results of CCK-8 assays indicated that Cytarabine, as well as these three molecule drugs, inhibits the proliferation of RCH-ACV cells. (B) The apoptosis-positive cells of RCH-ACV cells after drug treatment at different drug concentrations for 60 h by TUNEL staining (×200). (n ≥ 3, one-way ANOVA, mean±SEM, ns: no significance, *P< 0.05, **P< 0.01, ***P< 0.001, ****P< 0.0001).

Figure S1

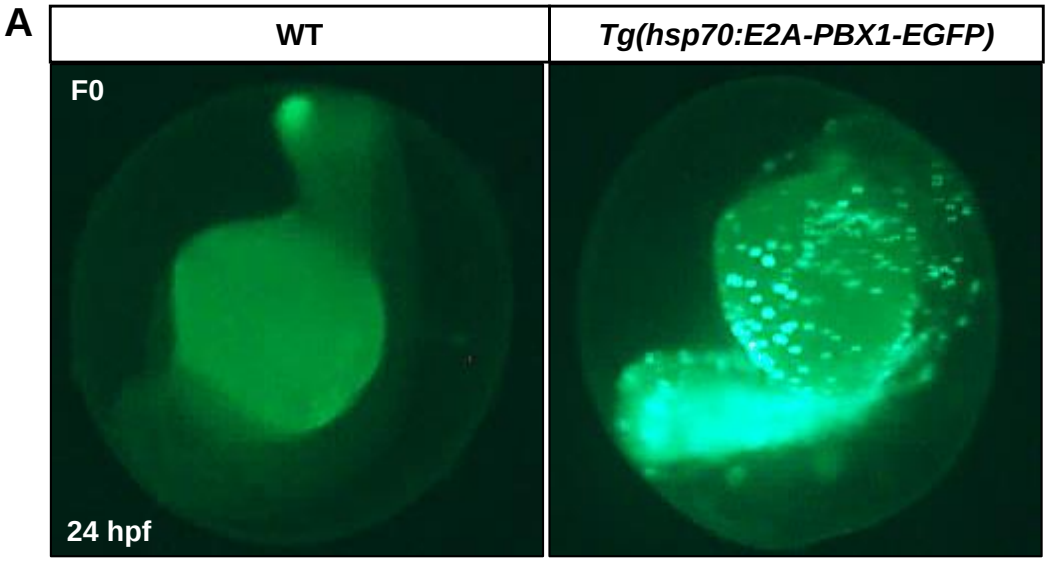
A
WT
Tg(hsp70:E2A-PBX1-EGFP)
F0
24 hpf

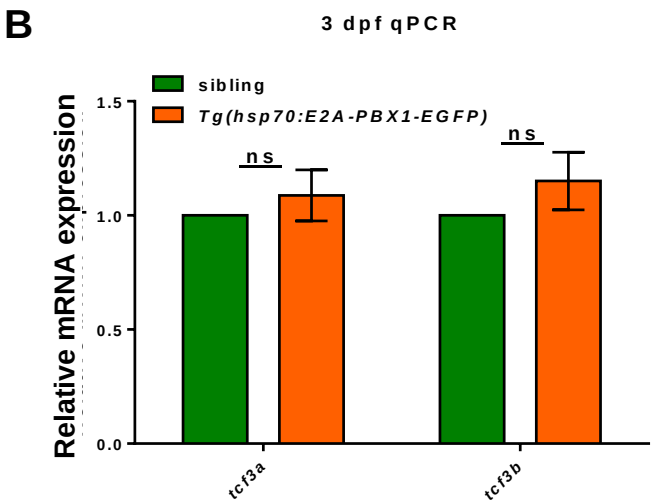
B
3 dpf qPCR
sibling
Tg(hsp70:E2A-PBX1-EGFP)
Relative mRNA expression
1.5
1.0
0.5
0.0
ns
ns
tcf3a
tcf3b

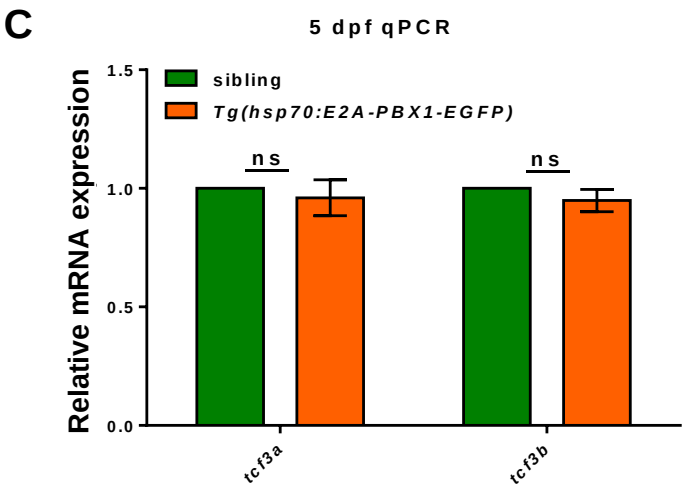
C
5 dpf qPCR
sibling
Tg(hsp70:E2A-PBX1-EGFP)
Relative mRNA expression
1.5
1.0
0.5
0.0
ns
ns
tcf3a
tcf3b

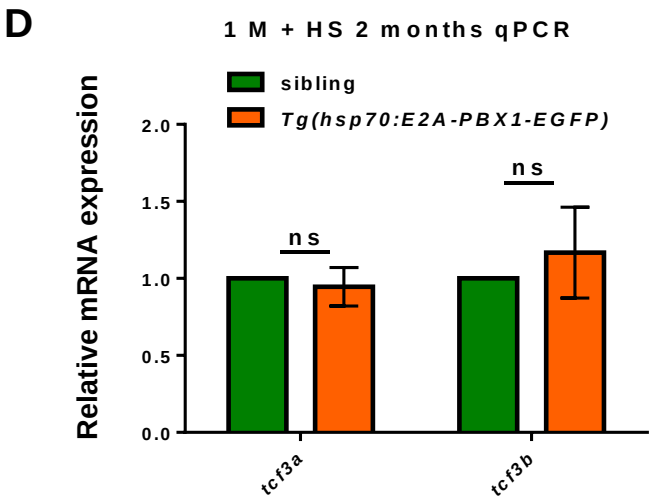
D
1 M + HS 2 months qPCR
sibling
Tg(hsp70:E2A-PBX1-EGFP)
Relative mRNA expression
2.0
1.5
1.0
0.5
0.0
ns
ns
tcf3a
tcf3b

Figure S2

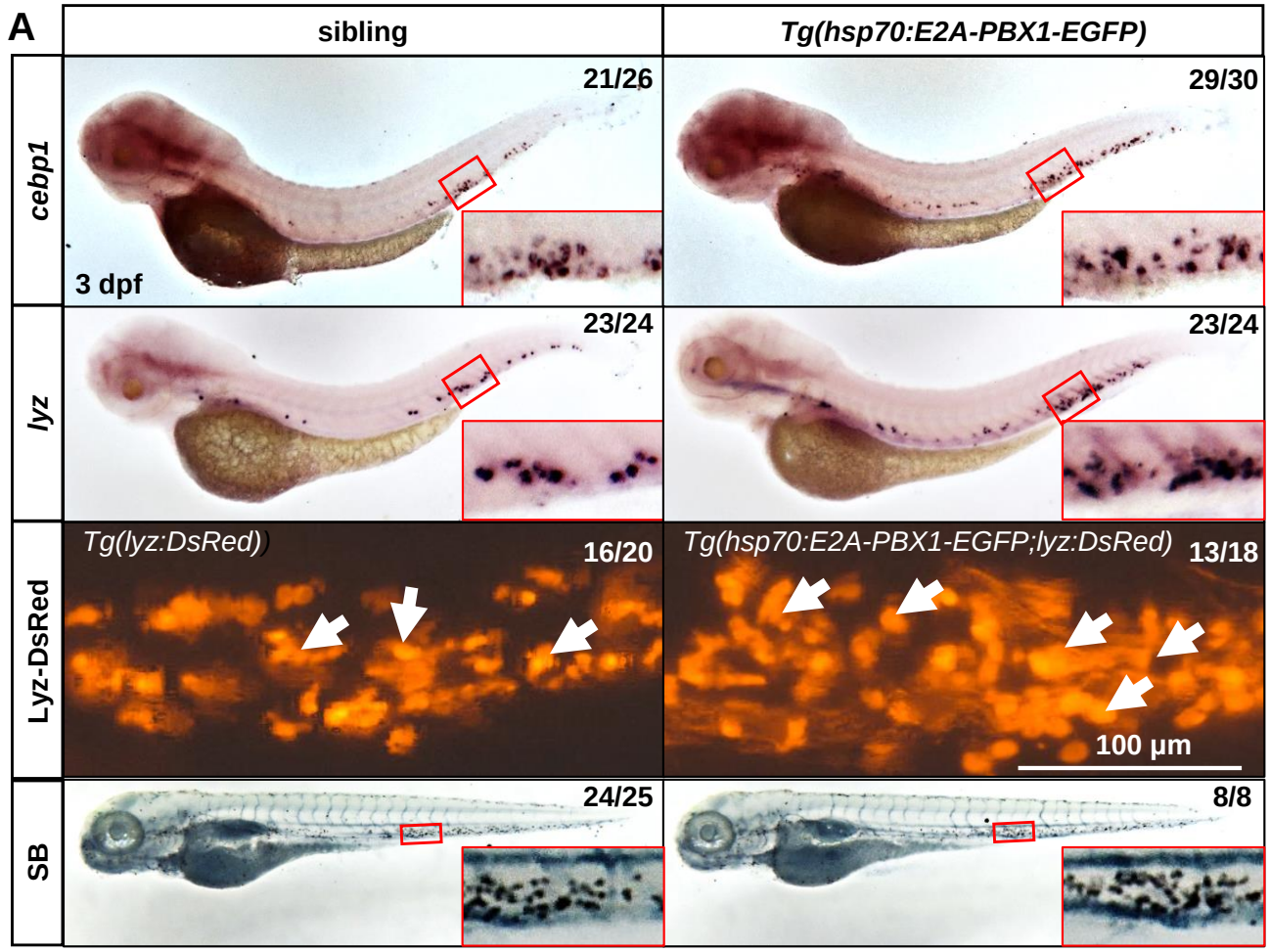
A
sibling
Tg(hsp70:E2A-PBX1-EGFP)
cebp1
21/26
29/30
3 dpf
lyz
23/24
23/24
Lyz-DsRed
Tg(lyz:DsRed)
16/20
Tg(hsp70:E2A-PBX1-EGFP;lyz:DsRed)
13/18
100 μm
SB
24/25
8/8

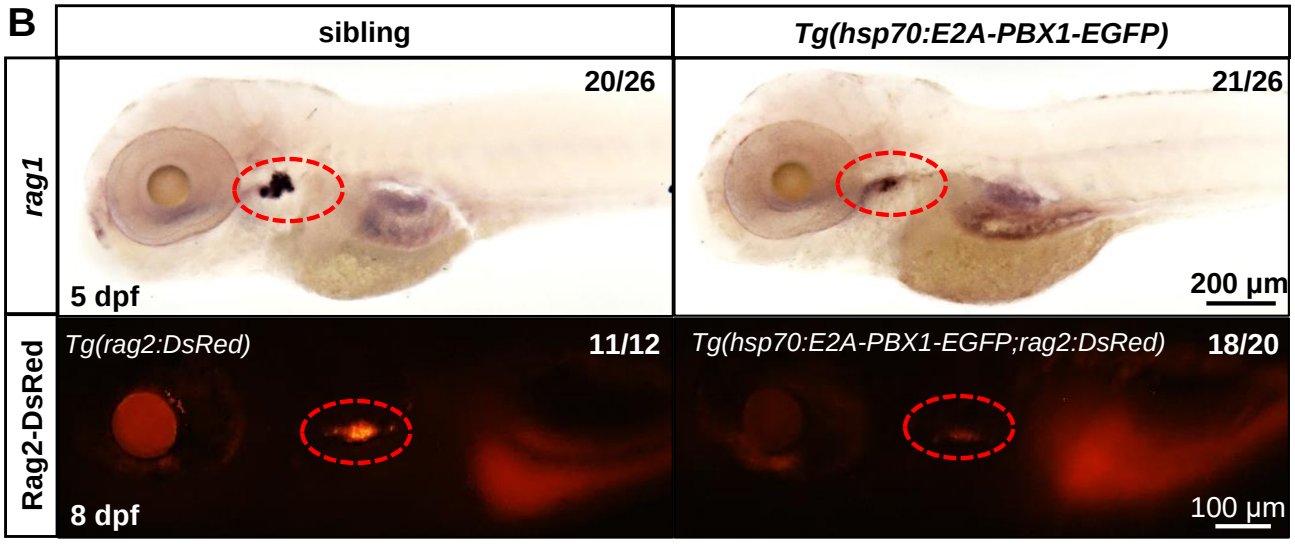
B
sibling
Tg(hsp70:E2A-PBX1-EGFP)
rag1
20/26
21/26
5 dpf
200 μm
Rag2-DsRed
Tg(rag2:DsRed)
11/12
Tg(hsp70:E2A-PBX1-EGFP;rag2:DsRed)
18/20
8 dpf
100 μm

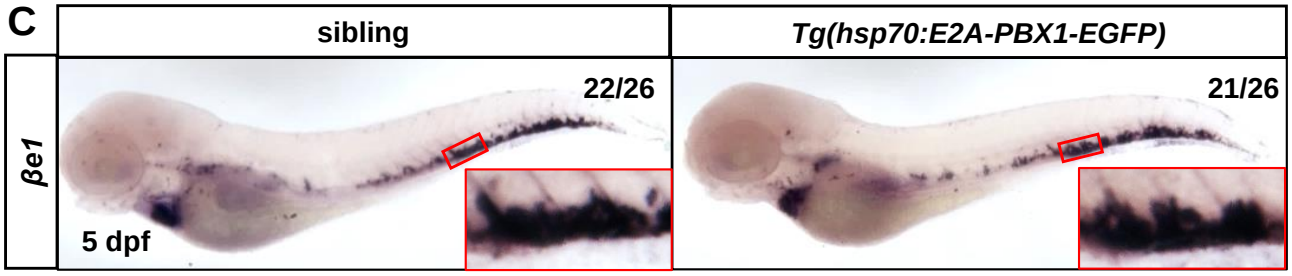
C
sibling
Tg(hsp70:E2A-PBX1-EGFP)
βe1
22/26
21/26
5 dpf

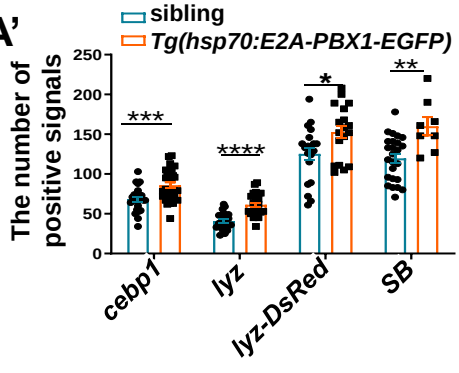
A'
sibling
Tg(hsp70:E2A-PBX1-EGFP)
The number of positive signals
***
****
*
**
cebp1
lyz
lyz-DsRed
SB

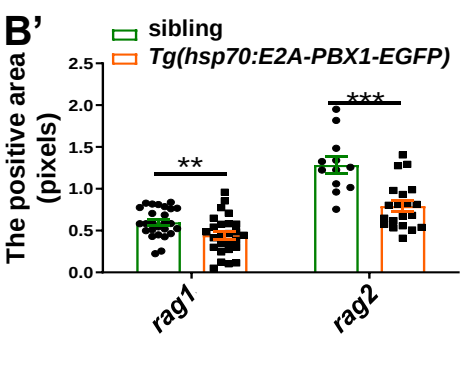
B'
sibling
Tg(hsp70:E2A-PBX1-EGFP)
The positive area (pixels)
**
***
rag1
rag2

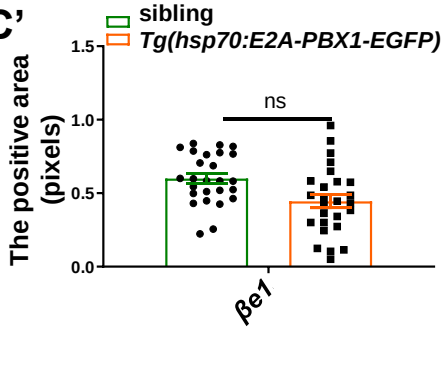
C'
sibling
Tg(hsp70:E2A-PBX1-EGFP)
The positive area (pixels)
ns
βe1

Figure S3

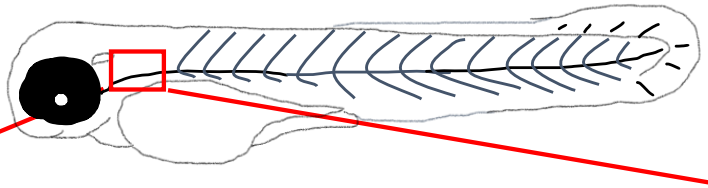

A

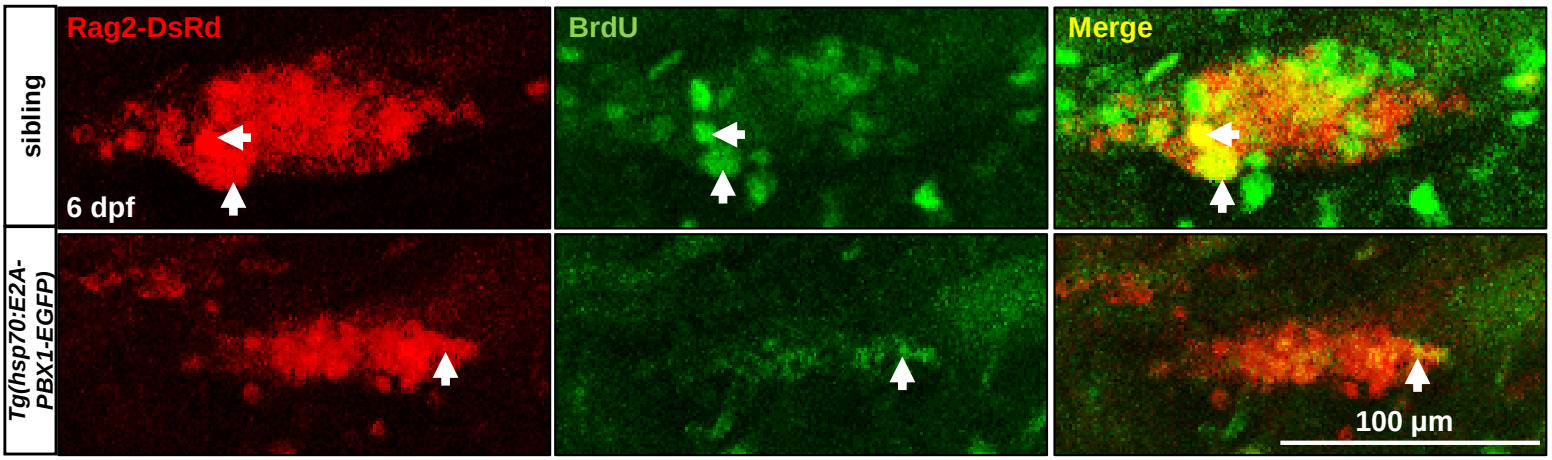

B

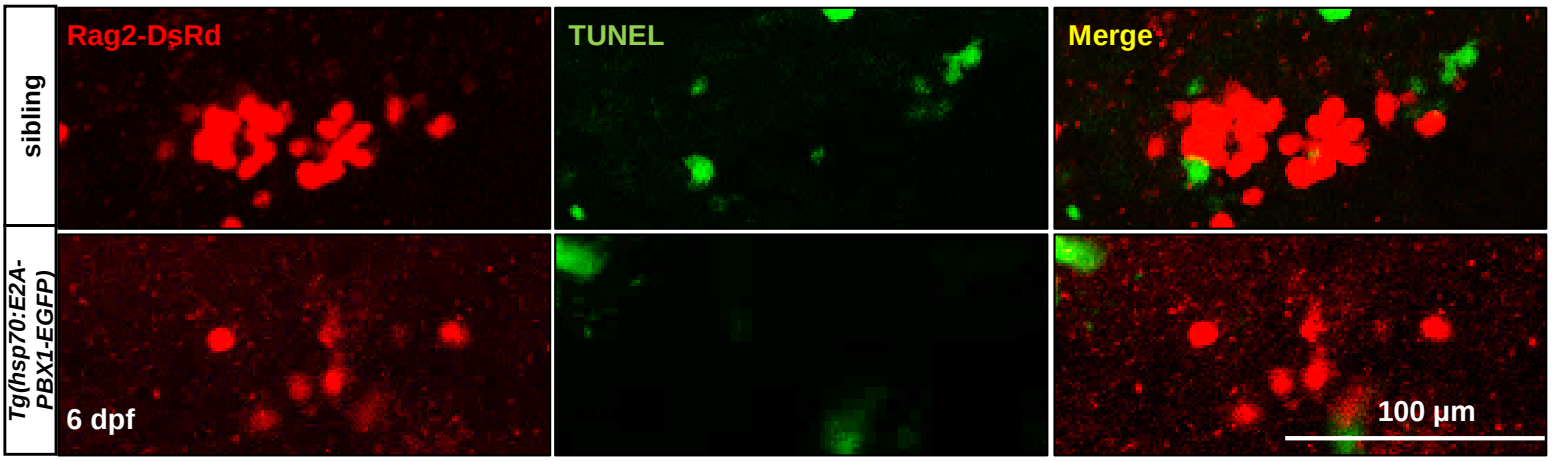

A'

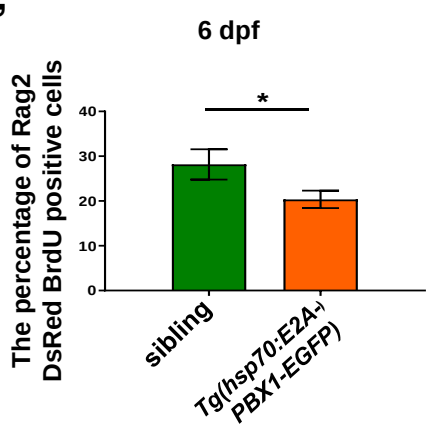

B'

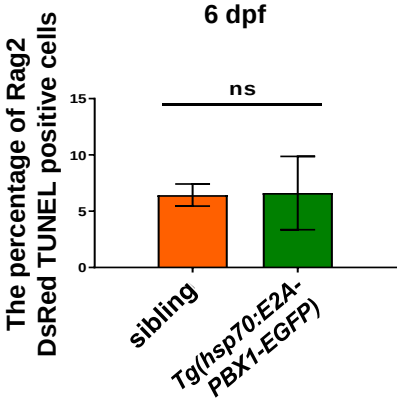

C

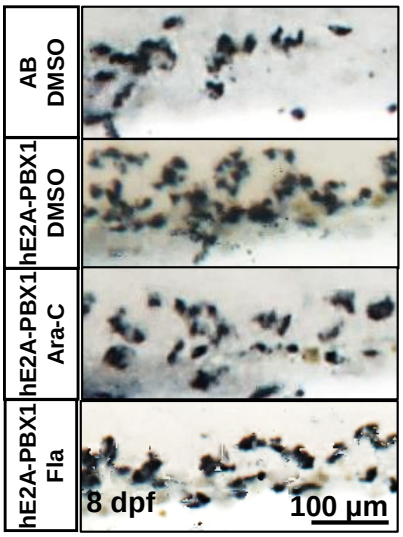

C'

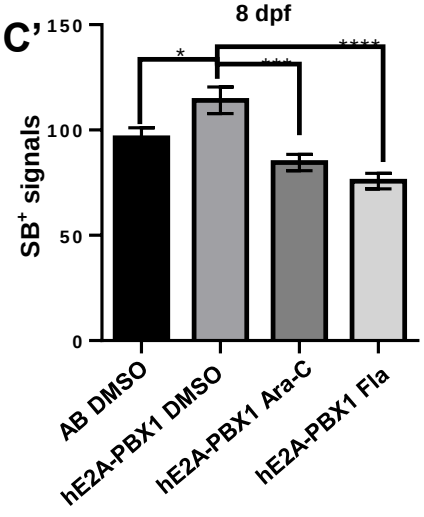

D

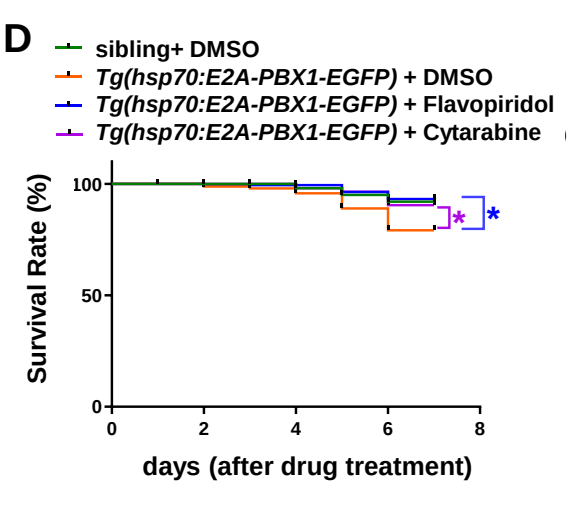

Figure S4

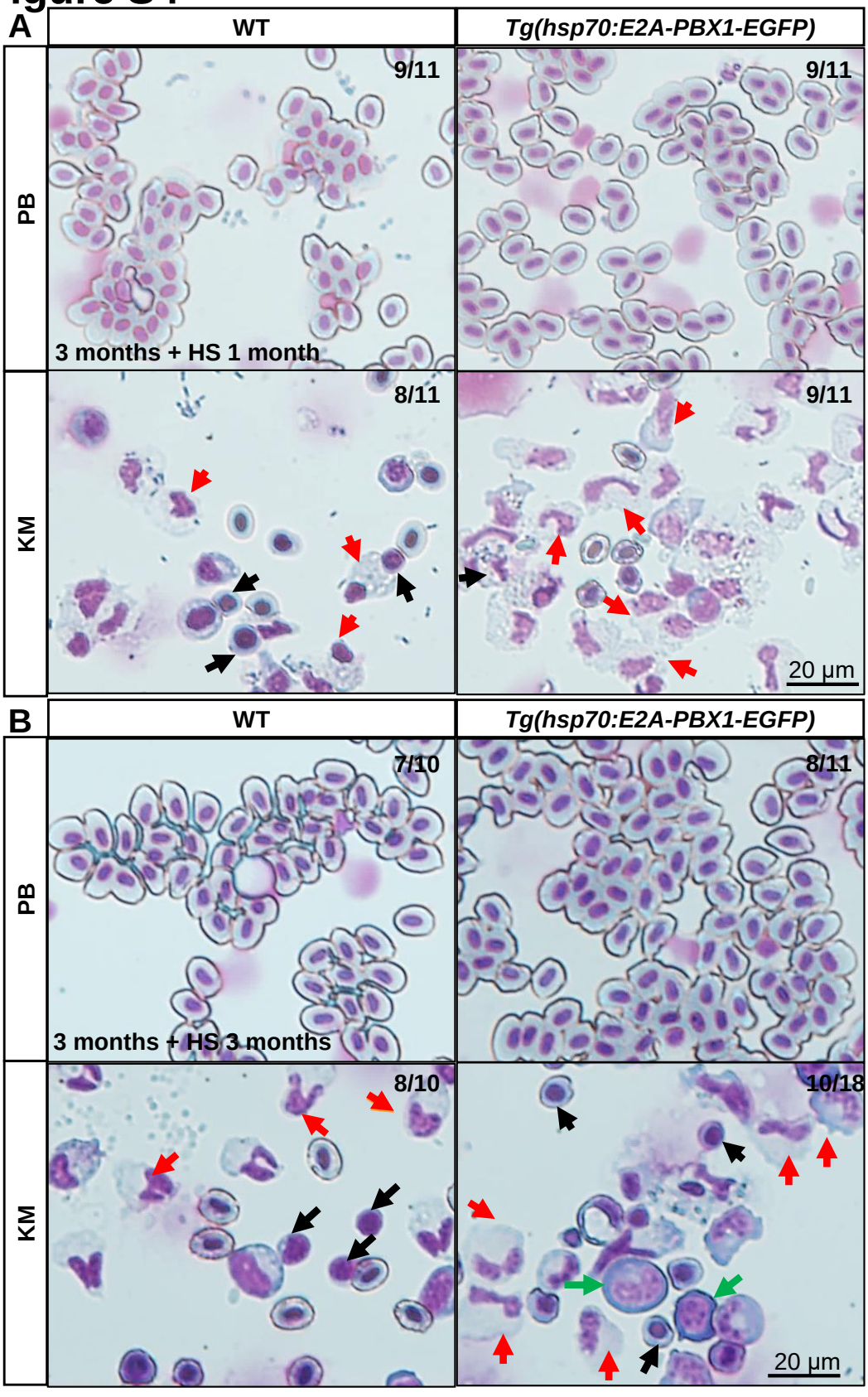

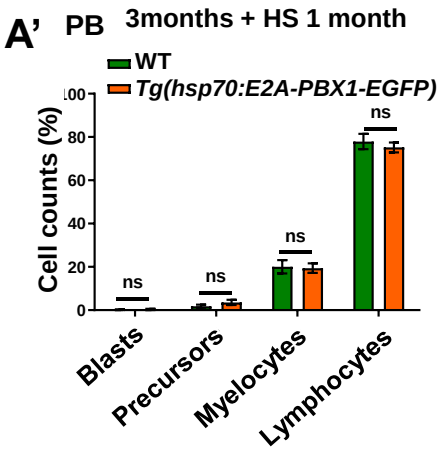

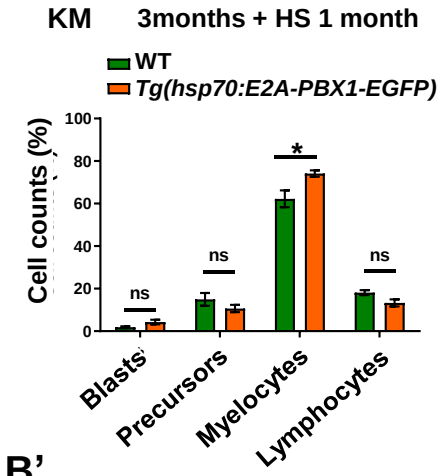

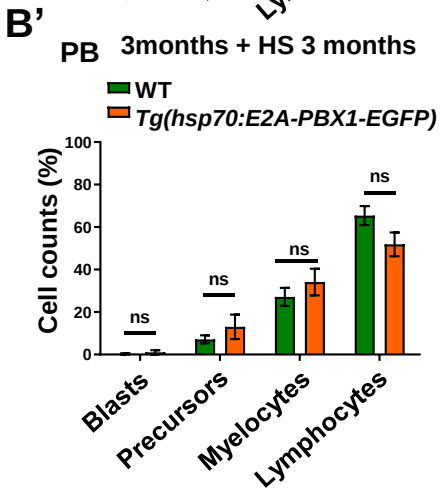

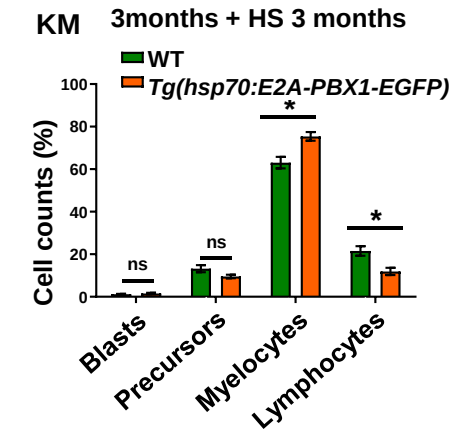

1 year + HS 3 months

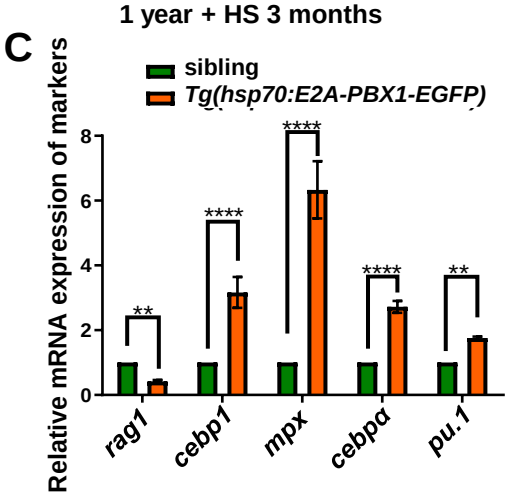

Figure S5

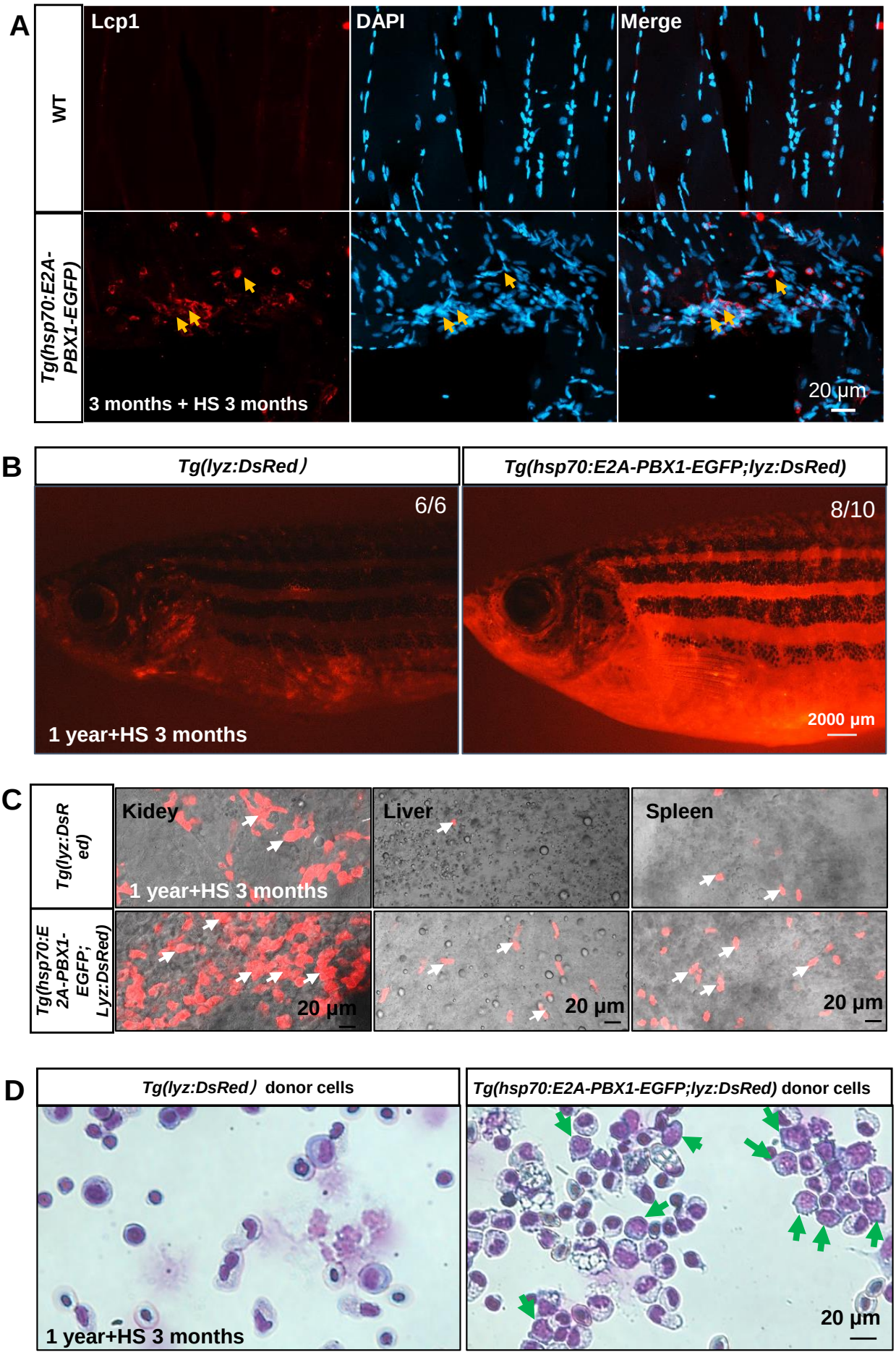
A
WT
Tg(hsp70:E2A-PBX1-EGFP)
Lcp1
DAPI
Merge
3 months + HS 3 months
20 μm
B
Tg(lyz:DsRed）
Tg(hsp70:E2A-PBX1-EGFP;lyz:DsRed)
6/6
8/10
1 year+HS 3 months
2000 μm
C
Tg(lyz:DsRed)
Tg(hsp70:E2A-PBX1-EGFP;Lyz:DsRed)
Kidey
Liver
Spleen
1 year+HS 3 months
20 μm
20 μm
20 μm
D
Tg(lyz:DsRed）donor cells
Tg(hsp70:E2A-PBX1-EGFP;lyz:DsRed) donor cells
1 year+HS 3 months
20 μm

Figure S6

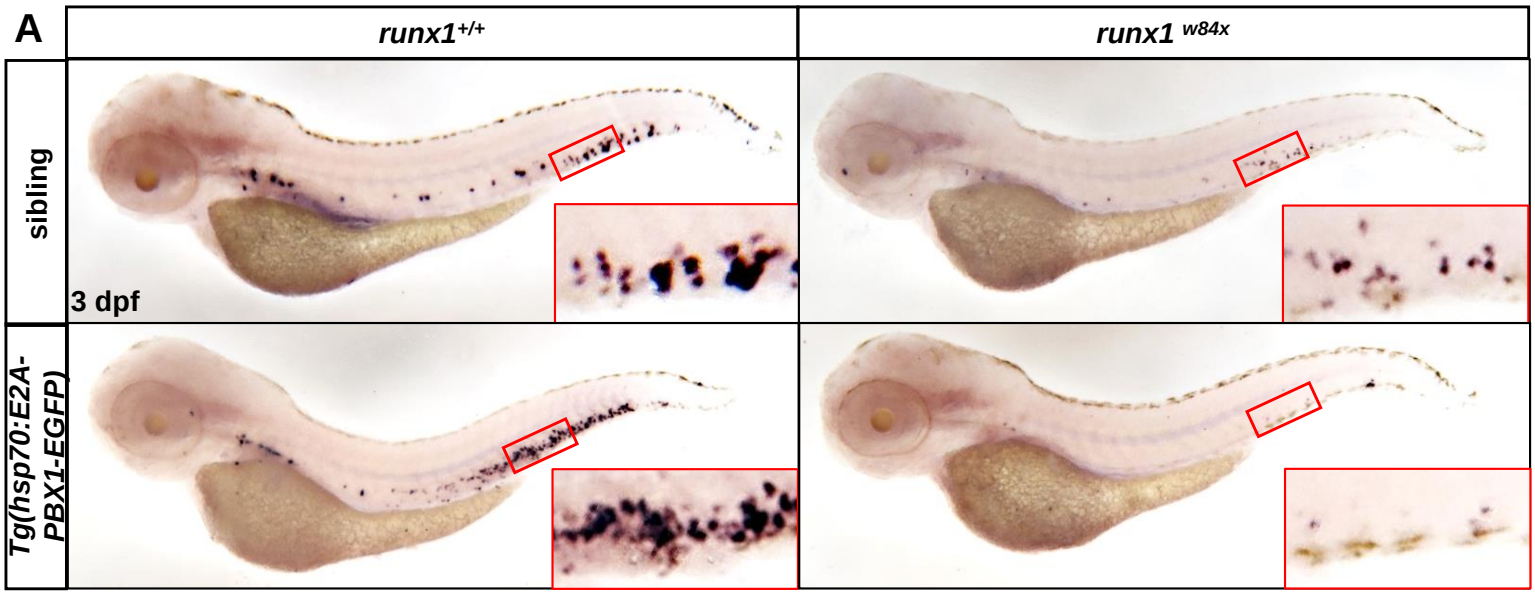
A
runx1+/+
runx1 w84x
sibling
Tg(hsp70:E2A-PBX1-EGFP)
3 dpf

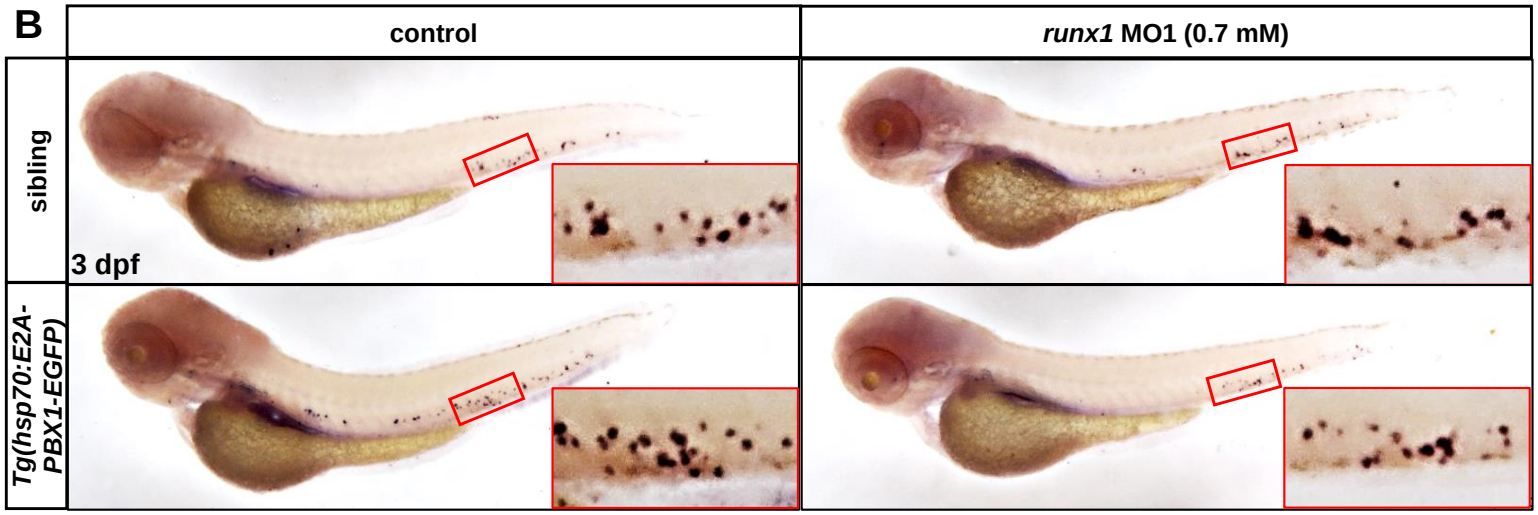
B
control
runx1 MO1 (0.7 mM)
sibling
Tg(hsp70:E2A-PBX1-EGFP)
3 dpf

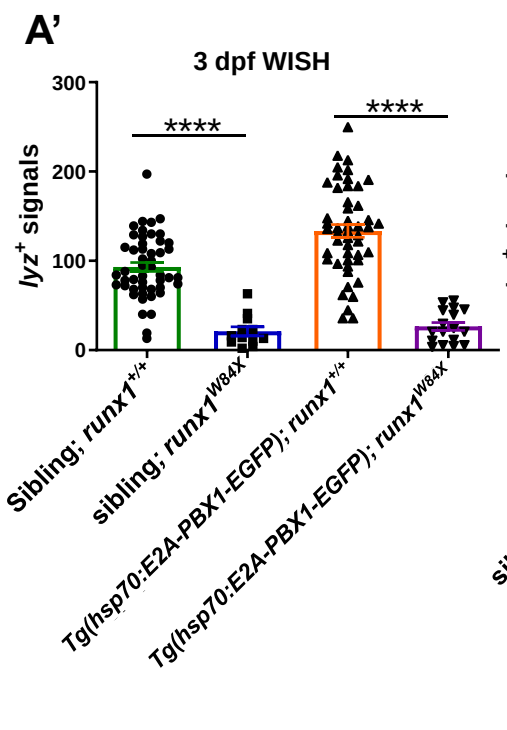
A'
3 dpf WISH
lyz+ signals
300
200
100
0
****
****
Sibling; runx1+/+
sibling; runx1W84X
Tg(hsp70:E2A-PBX1-EGFP); runx1+/+
Tg(hsp70:E2A-PBX1-EGFP); runx1W84X

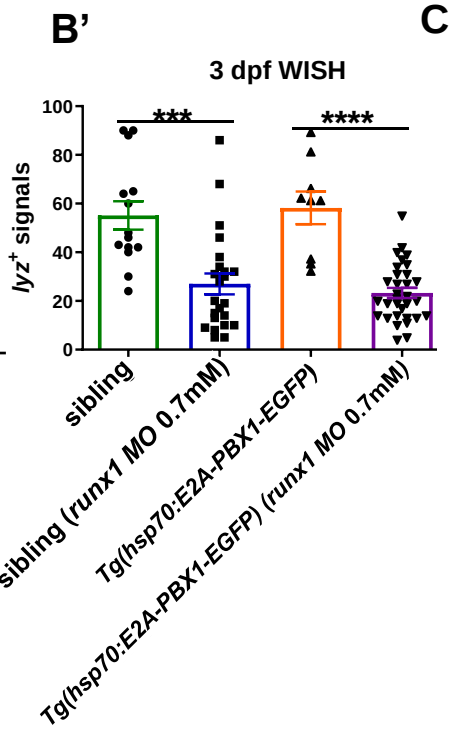
B'
3 dpf WISH
lyz+ signals
100
80
60
40
20
0
***
****
sibling
sibling (runx1 MO 0.7mM)
Tg(hsp70:E2A-PBX1-EGFP)
Tg(hsp70:E2A-PBX1-EGFP) (runx1 MO 0.7mM)

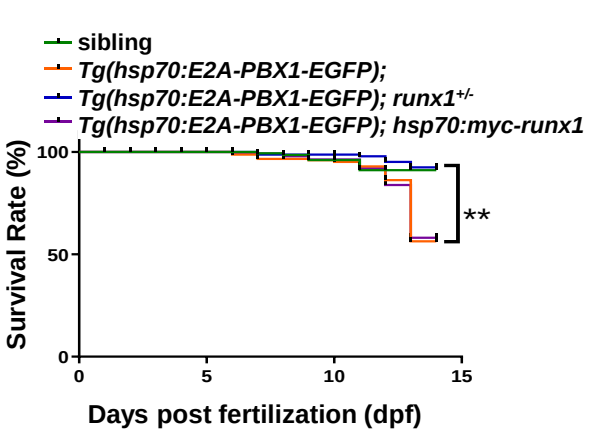
C
sibling
Tg(hsp70:E2A-PBX1-EGFP);
Tg(hsp70:E2A-PBX1-EGFP); runx1+/-
Tg(hsp70:E2A-PBX1-EGFP); hsp70:myc-runx1
Survival Rate (%)
100
50
0
0
5
10
15
**
Days post fertilization (dpf)

Figure S7

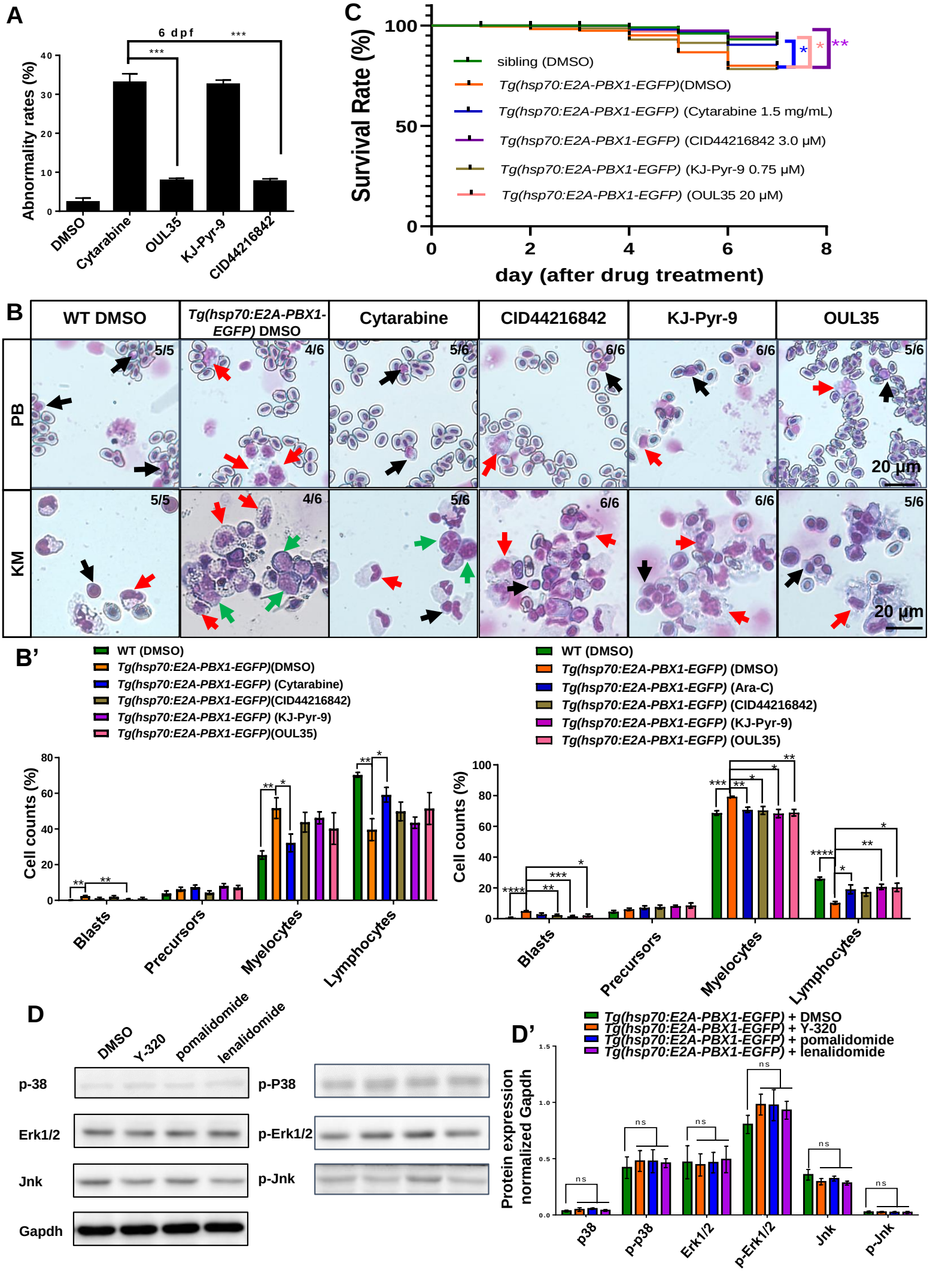
A
6 dpf
***
***
Abnormality rates (%)
40
30
20
10
0
DMSO
Cytarabine
OUL35
KJ-Pyr-9
CID44216842
C
Survival Rate (%)
100
50
0
0
2
4
6
8
day (after drug treatment)
sibling (DMSO)
Tg(hsp70:E2A-PBX1-EGFP)(DMSO)
Tg(hsp70:E2A-PBX1-EGFP) (Cytarabine 1.5 mg/mL)
Tg(hsp70:E2A-PBX1-EGFP) (CID44216842 3.0 μM)
Tg(hsp70:E2A-PBX1-EGFP) (KJ-Pyr-9 0.75 μM)
Tg(hsp70:E2A-PBX1-EGFP) (OUL35 20 μM)
B
WT DMSO
Tg(hsp70:E2A-PBX1-EGFP) DMSO
Cytarabine
CID44216842
KJ-Pyr-9
OUL35
PB
KM
5/5
4/6
5/6
6/6
6/6
5/6
20 μm
B'
WT (DMSO)
Tg(hsp70:E2A-PBX1-EGFP)(DMSO)
Tg(hsp70:E2A-PBX1-EGFP) (Cytarabine)
Tg(hsp70:E2A-PBX1-EGFP)(CID44216842)
Tg(hsp70:E2A-PBX1-EGFP) (KJ-Pyr-9)
Tg(hsp70:E2A-PBX1-EGFP)(OUL35)
Cell counts (%)
Blasts
Precursors
Myelocytes
Lymphocytes
WT (DMSO)
Tg(hsp70:E2A-PBX1-EGFP) (DMSO)
Tg(hsp70:E2A-PBX1-EGFP) (Ara-C)
Tg(hsp70:E2A-PBX1-EGFP) (CID44216842)
Tg(hsp70:E2A-PBX1-EGFP) (KJ-Pyr-9)
Tg(hsp70:E2A-PBX1-EGFP) (OUL35)
Cell counts (%)
Blasts
Precursors
Myelocytes
Lymphocytes
D
DMSO
Y-320
pomalidomide
lenalidomide
p-38
p-P38
Erk1/2
p-Erk1/2
Jnk
p-Jnk
Gapdh
D'
Tg(hsp70:E2A-PBX1-EGFP) + DMSO
Tg(hsp70:E2A-PBX1-EGFP) + Y-320
Tg(hsp70:E2A-PBX1-EGFP) + pomalidomide
Tg(hsp70:E2A-PBX1-EGFP) + lenalidomide
Protein expression normalized Gapdh
ns
p38
p-p38
Erk1/2
p-Erk1/2
Jnk
p-Jnk

Figure S8

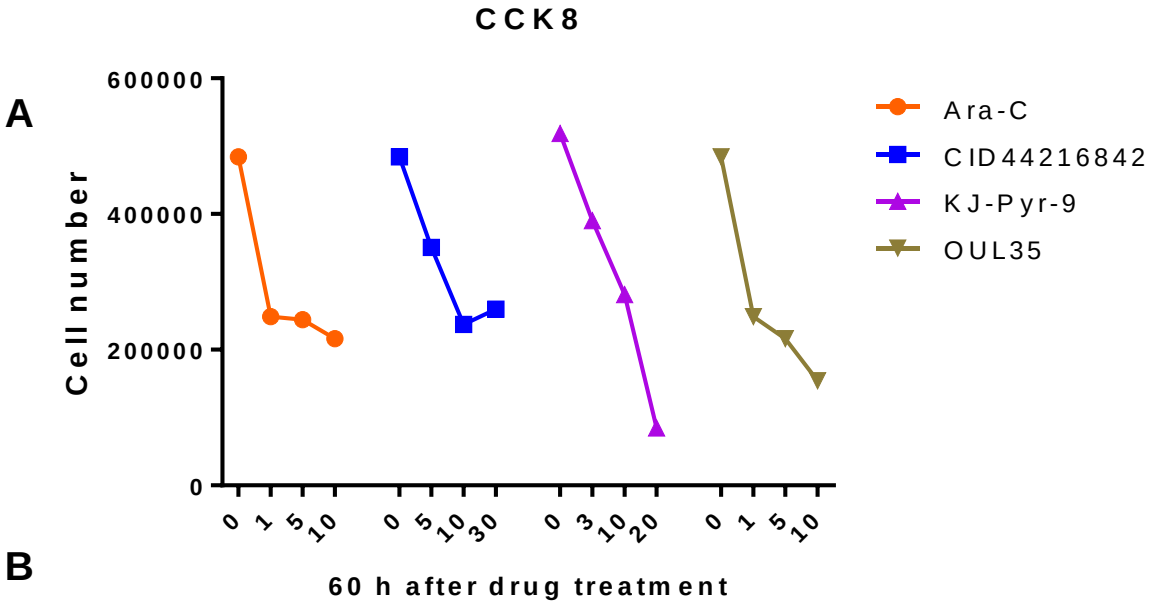
A
CCK8
Cell number
600000
400000
200000
0
0 1 5 10
0 5 10 30
0 3 10 20
0 1 5 10
60 h after drug treatment
Ara-C
CID44216842
KJ-Pyr-9
OUL35

B

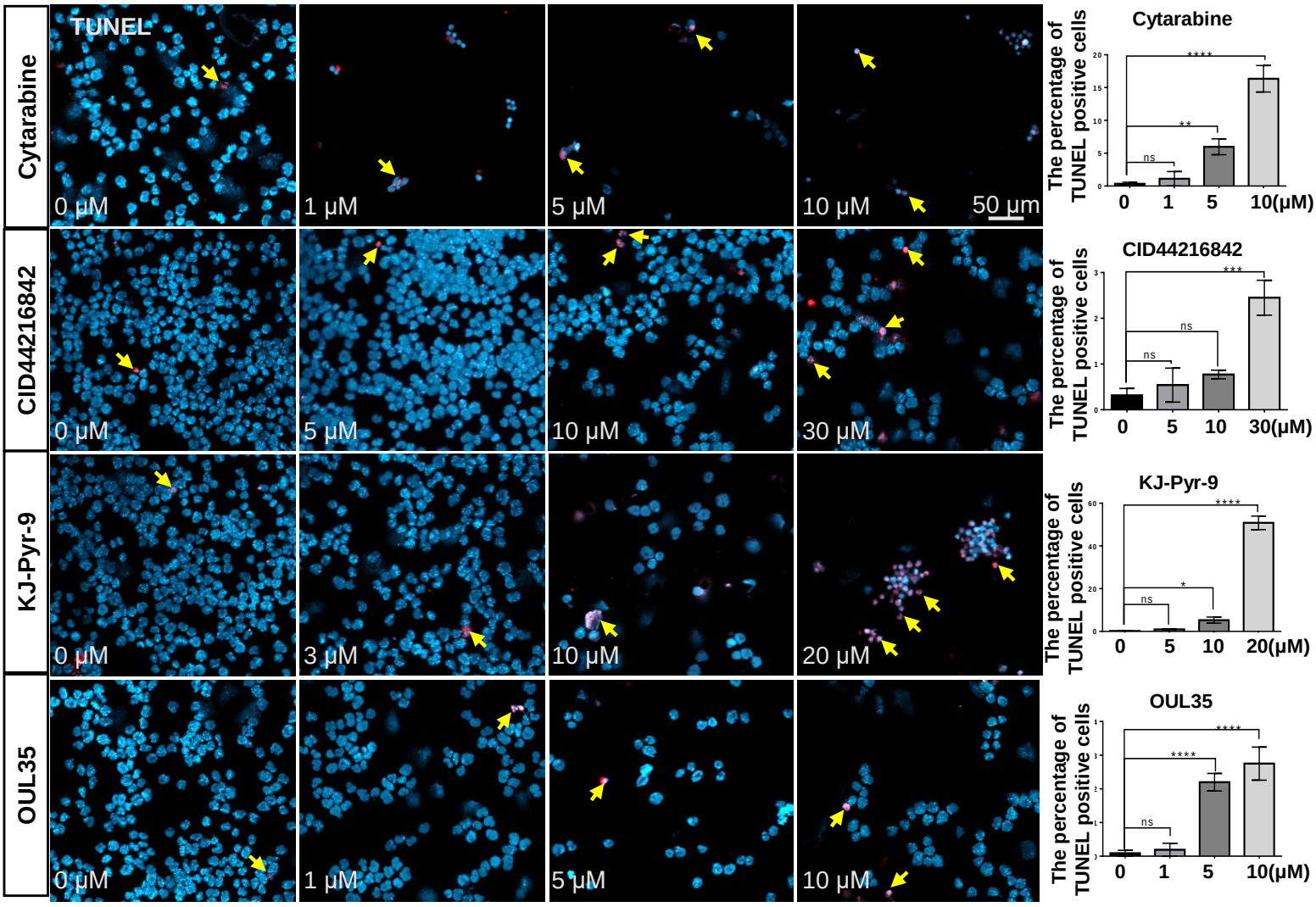
Cytarabine
TUNEL
0 μM
1 μM
5 μM
10 μM
50 μm
CID44216842
0 μM
5 μM
10 μM
30 μM
KJ-Pyr-9
0 μM
3 μM
10 μM
20 μM
OUL35
0 μM
1 μM
5 μM
10 μM
The percentage of TUNEL positive cells
Cytarabine
0 1 5 10(μM)
CID44216842
0 5 10 30(μM)
KJ-Pyr-9
0 5 10 20(μM)
OUL35
0 1 5 10(μM)
ns
**
***
****
*

References:

1. Westerfield M. The Zebrafish Book: A Guide for the Laboratory Use of Zebrafish (Danio Rerio): University of Oregon Press, 2000.
2. Jin H, Sood R, Xu J, et al. Definitive hematopoietic stem/progenitor cells manifest distinct differentiation output in the zebrafish VDA and PBI. Development. 2009;136(4):647-654.
3. Hall C, Flores MV, Storm T, Crosier K, Crosier P. The zebrafish lysozyme C promoter drives myeloid-specific expression in transgenic fish. BMC Dev Biol. 2007; 7(1): 1-17.
4. Willett CE, Cherry JJ, Steiner LA. Characterization and expression of the recombination activating genes (rag1 and rag2) of zebrafish. Immunogenetics. 1997;45(6):394-404.
5. Jin H, Li L, Xu J, et al. Runx1 regulates embryonic myeloid fate choice in zebrafish through a negative feedback loop inhibiting Pu.1 expression. Blood. 2012;119(22):5239-5249.
6. Chitramuthu BP, Bennett HP. High resolution whole mount in situ hybridization within zebrafish embryos to study gene expression and function. J Vis Exp. 2013;80:e50644.
7. Qian F, Zhen F, Xu J, Huang M, Li W, Wen Z. Distinct functions for different scl isoforms in zebrafish primitive and definitive hematopoiesis. PLoS Biol. 2007;5(5):e132.
8. Alghisi E, Distel M, Malagola M, et al. Targeting oncogene expression to endothelial cells induces proliferation of the myelo-erythroid lineage by repressing the Notch pathway. Leukemia. 2013;27(11):2229-2241.
9. Xue S, Zhou F, Zhao T, et al. Phase separation on cell surface facilitates bFGF signal transduction with heparan sulphate. Nat Commun. 2022;13(1):1112.
10. Hart JR, Garner AL, Yu J, et al. Inhibitor of MYC identified in a Krohnke pyridine library. Proc Natl Acad Sci U S A. 2014;111(34):12556-12561.
11. Mandal JP, Shiue CN, Chen YC, et al. PKCdelta mediates mitochondrial ROS generation and oxidation of HSP60 to relieve RKIP inhibition on MAPK pathway for HCC progression. Free Radic Biol Med. 2021;163(69-87).
12. Tian Y, Korn P, Tripathi P, et al. The mono-ADP-ribosyltransferase ARTD10 regulates the voltage-gated K(+) channel Kv1.1 through protein kinase C delta. BMC Biol. 2020;18(1):143.
13. Vergnani L, Hatrik S, Ricci F, et al. Effect of native and oxidized low-density lipoprotein on endothelial nitric oxide and superoxide production : key role of L-arginine availability. Circulation. 2000;101(11):1261-1266.
14. Chen Z, Gopalakrishnan SM, Bui MH, et al. 1-Benzyl-3-cetyl-2-methylimidazolium iodide (NH125) induces phosphorylation of eukaryotic elongation factor-2 (eEF2): a cautionary note on the anticancer mechanism of an eEF2 kinase inhibitor. J Biol Chem. 2011;286(51):43951-43958.
15. Downward J. Targeting RAS signalling pathways in cancer therapy. Nat Rev Cancer. 2003;3(1):11-22.
16. Hong L, Kenney SR, Phillips GK, et al. Characterization of a Cdc42 protein inhibitor and its use as a molecular probe. J Biol Chem. 2013;288(12):8531-8543.
17. Van der Plas SE, Kelgtermans H, De Munck T, et al. Discovery of N-(3-Carbamoyl-5,5,7,7-tetramethyl-5,7-dihydro-4H-thieno[2,3-c]pyran-2-yl)-lH-pyrazole-5-carboxam ide (GLPG1837), a Novel Potentiator Which Can Open Class III Mutant Cystic Fibrosis Transmembrane Conductance Regulator (CFTR) Channels to a High Extent. J Med Chem. 2018;61(4):1425-1435.
18. Deng X, Dzamko N, Prescott A, et al. Characterization of a selective inhibitor of the Parkinson's disease kinase LRRK2. Nat Chem Biol. 2011;7(4):203-205.

19. Banks KM, Lan Y, Evans T. Tet Proteins Regulate Neutrophil Granulation in Zebrafish through Demethylation of socs3b mRNA. Cell Rep. 2021;34(2):108632.
20. Zhang MQ, Chen B, Zhang JP, Chen N, Liu CZ, Hu CQ. Liver toxicity of macrolide antibiotics in zebrafish. Toxicology. 2020;441:152501.
21. Mao L, Bryantsev AL, Chechenova MB, Shelden EA. Cloning, characterization, and heat stress-induced redistribution of a protein homologous to human hsp27 in the zebrafish Danio rerio. Exp Cell Res. 2005;306(1):230-241.
22. Koizumi SI, Sasaki D, Hsieh TH, et al. JunB regulates homeostasis and suppressive functions of effector regulatory T cells. Nat Commun. 2018;9(1):5344.
23. Silva NJ, Nagashima M, Li J, et al. Inflammation and matrix metalloproteinase 9 (Mmp-9) regulate photoreceptor regeneration in adult zebrafish. Glia. 2020;68(7):1445-1465.
24. Han R, Wang R, Zhao Q, et al. Trim69 regulates zebrafish brain development by ap-1 pathway. Sci Rep. 2016;6:24034.
25. Hu W, Yang S, Shimada Y, et al. Infection and RNA-seq analysis of a zebrafish tlr2 mutant shows a broad function of this toll-like receptor in transcriptional and metabolic control and defense to Mycobacterium marinum infection. BMC Genomics. 2019;20(1):878.